A Series of Metal-Organic Frameworks Based on 5-(4-Pyridyl)-Isophthalic Acid: Selective Sorption and Fluorescence Sensing

Xiaofang Zheng,[†,§] *Li Zhou,*[†,§] *Yumei Huang,*[†] *Chenggang Wang,*[†] *Jingui Duan,*[‡] *Lili Wen,*[*,†] *Zhengfang Tian*[&] *and Dongfeng Li*[*,†]

[†]Key Laboratory of Pesticide & Chemical Biology of Ministry of Education, College of Chemistry, Central China Normal University, Wuhan, 430079, P. R. China.

[‡] State Key Laboratory of Materials-Oriented Chemical Engineering, Nanjing University of Technology, Nanjing, 210009, P. R. China.

[&] Hubei Key Laboratory for Processing and Application of Catalytic Materials, Huanggang Normal University, Huangguang, 438000, P. R. China.

[§]Xiaofang Zheng and Li Zhou contributed equally to this work

Table S1. Selected Bond Distances (Å) and Angles (deg) for **1**-**4**.

		1[a]	
Ni1−O3	1.980(3)	Ni1−O5	2.085(4)
Ni1−O6	2.132(3)	Ni1−O4#1	2.058(3)
Ni1−N1#2	2.066(4)	Ni1−O1#3	1.984(3)
O1#3 −Ni1−O3	172.75(15)	O4#1−Ni1−O5	176.65(13)
O6 −Ni1−N1#2	178.17(10)		
		2[b]	
Ni1−O1	2.099(2)	Ni1−O1W	2.141(3)
Ni1−O4W	2.098(3)	Ni1−O10	2.055(2)
Ni1−N2	2.067(3)	Ni1−O4#1	1.961(2)
Ni2−O1W	2.140(2)	Ni2−O5W	2.084(2)
Ni2−O9	1.994(3)	Ni2−O13	1.998(3)
Ni2−O3#1	1.959(3)	Ni2−N3#2	2.090(3)

Ni3−O2W	2.136(2)	Ni3−O15	2.085(2)
Ni3−O17	1.981(2)	Ni3−O25	2.054(2)
Ni3−O19#1	1.999(2)	Ni3−N5#3	2.094(3)
Ni4−O2W	2.130(2)	Ni4−O6W	2.091(2)
Ni4−O16	1.996(2)	Ni4−O21	2.021(3)
Ni4−O20#1	2.037(2)	Ni4−N6#4	2.099(3)
Ni5−O3W	2.135(2)	Ni5−O7W	2.237(3)
Ni5−O24	2.014(3)	Ni5−O12#5	1.972(3)
Ni5−O7#6	2.067(3)	Ni5−N4#4	2.086(3)
Ni6−O3W	2.186(3)	Ni6−O23	2.050(3)
Ni6−N7	2.086(3)	Ni6 −O8#6	1.998(2)
Ni6−O5#3	1.995(2)	Ni6−N1#3	2.116(3)
O1W−Ni1−N2	177.05(11)	O4W−Ni1−O10	176.74(10)
O1−Ni1−O4#1	161.27(10)	O9−Ni2 −O13	175.41(10)
O1W−Ni2−N3#2	177.68(11)	O3#1−Ni2−O5W	175.59(10)
O15−Ni3−O25	175.40(10)	O2W−Ni3−N5#3	177.74(11)
O17−Ni3−O19#1	172.72(10)	O2W−Ni4−N6#4	178.19(11)
O6W−Ni4−O20#1	177.82(10)	O16−Ni4 −O21	172.86(10)
O3W−Ni5−N4#4	177.19(11)	O7#6−Ni5−O7W	175.37(10)
O12#5−Ni5−O24	174.30(11)	O3W−Ni6−N1#3	175.48(11)
O23−Ni6−N7	179.43(12)	O5#3−Ni6−O8#6	174.06(11)
		3[c]	
Co1−N1	2.129(3)	Co1−N5	2.148(3)
Co1−O4#1	2.155(3)	Co1−O7#2	2.096(3)
Co1−N10#3	2.194(3)	Co2−O1	2.055(3)
Co2−O5	2.039(3)	Co2−N8	2.121(3)
Co2−N4#4	2.135(3)	Co2−N9#5	2.140(3)
N1−Co1−N5	173.58(12)	O4#1−Co1−N10#3	140.93(10)
O7#2−Co1−N10#3	131.87(10)		
		4[d]	
Zn1−O1	2.002(4)	Zn1−N1	2.052(7)
Zn1−N2	1.999(6)	Zn1−O1#1	2.002(4)
O1−Zn1−N1	101.72(18)	O1#1 −Zn1−N2	110.89(17)

[a] Symmetry codes for **1**: #1 2-*x*, *y*, 1/2-*z*; #2 2-*x*, -*y*, -*z*; #3 1/2+*x*, 1/2+*y*, *z*

[b] Symmetry codes for **2**: #1 -1+*x*, *y*, *z*; #2 -*x*, -*y*, -*z*; #3 1-*x*, -*y*, 1-*z*; #4 -*x*, 1-*y*, 1-*z*; #5 *x*, 1+*y*, 1+*z*; #6 -*x*, -*y*, 1-*z*

[c] Symmetry codes for **3**: #1 *x*, *y*, 1+*z*; #2 1+*x*, *y*, 1+*z*; #3 1-*x*, 1/2+*y*, 3/2-*z*; #4 -1+*x*, *y*, -2+*z*; #5 1-*x*,

1/2+*y*, 1/2-*z*

[d] Symmetry codes for **4**: #1 *x*, *y*, 2-*z*

Table S2. The kinetic diameter of the adsorbents and their maximum uptakes for activated **3**.

molecules	kinetic diameter (Å)	Uptake ($cm^3\ g^{-1}$)
water	2.64 – 2.9	125
methanol	3.626 – 4.0	70
ethanol	4.3 – 4.53	42
n-propanol	4.7	27
i-propanol	4.7	18

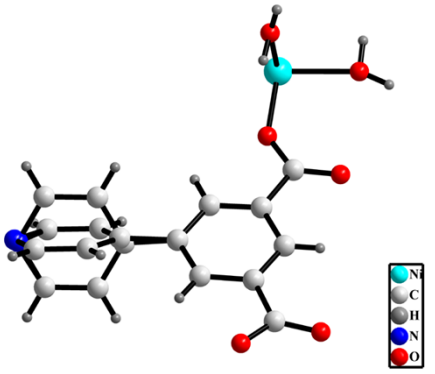

(a)

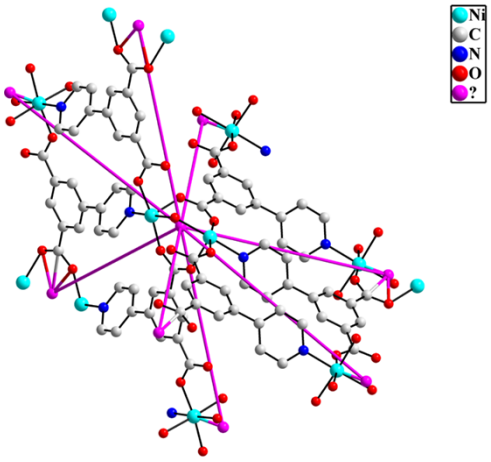

(b)

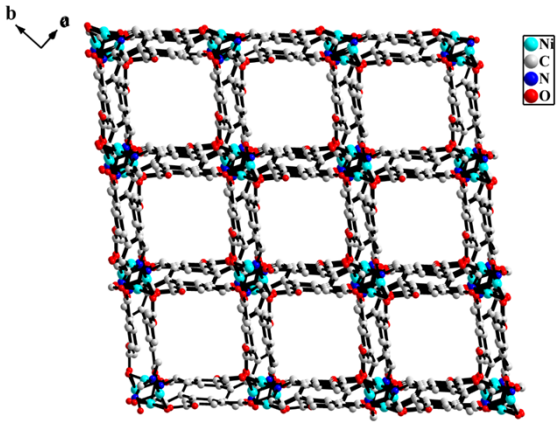

(c)

Figure S1. (a) The asymmetric unit of **1**, (b) coordination environment of dimmer unit [$Ni_2(COO)_2(\mu^2$-$H_2O)$] (violet), viewed as 8-connected node, (c) 3D framework of **1** along [1 1 0] directions.

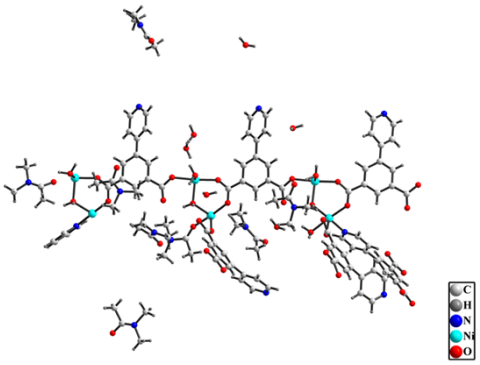

(a)

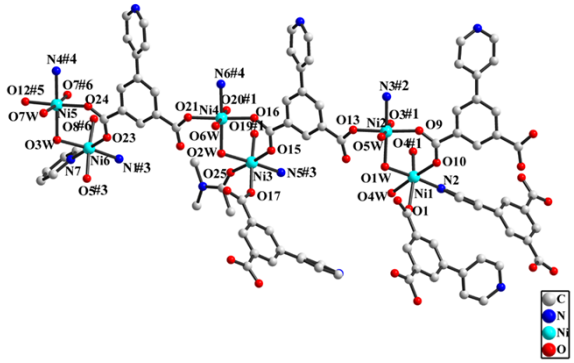

(b)

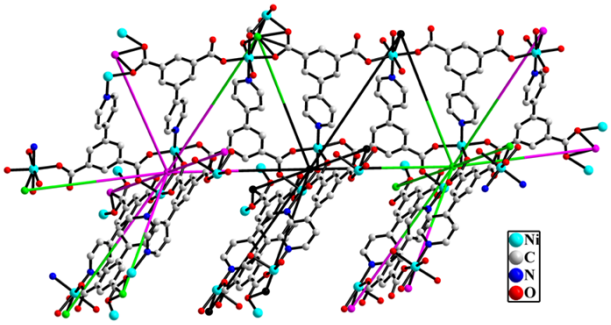

(c)

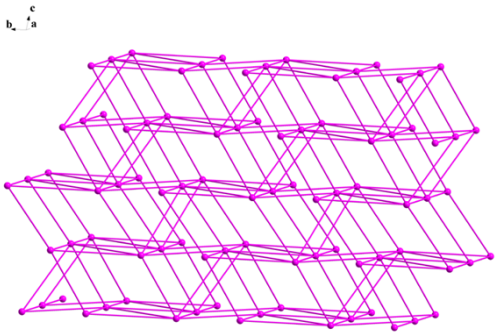

(d)

Figure S2. (a) The asymmetric unit of **2**, (b) coordination environment of Ni atom with hydrogen atoms omitted for clarity of **2**, (c) coordination environment of dimmer unit [$Ni_2(COO)_2(\mu^2$-$H_2O)$] (violet, green and black), viewed as 8-connected node, (d) the topological representation of **2**.

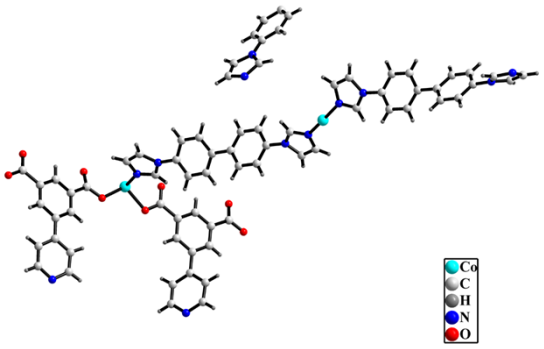

(a)

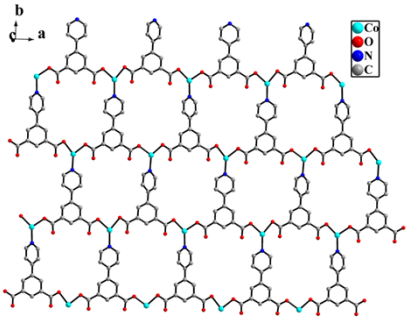

(b)

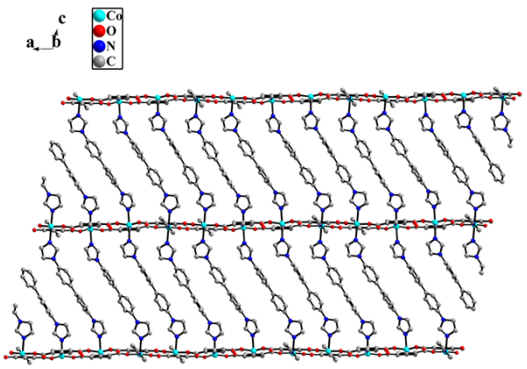

(c)

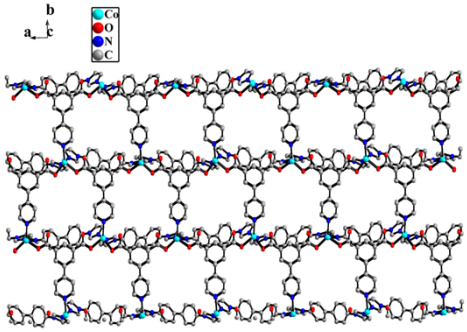

(d)

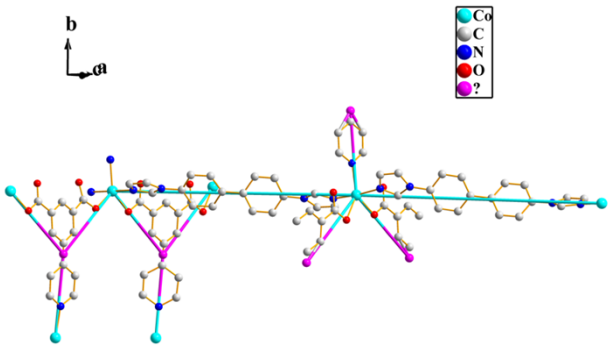

(e)

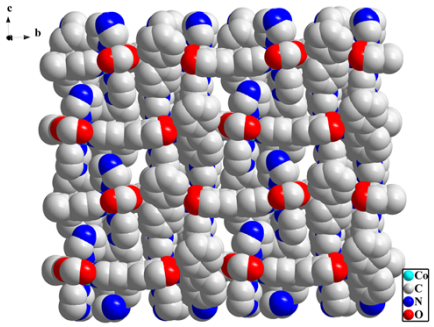

(f)

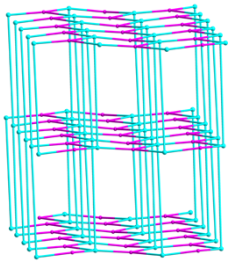

(g)

Figure S3. (a) The asymmetric unit of **3**, (b) 2D layer constructed from $pbdc^{2-}$ moiety and Co(II) atoms in **3**, (c) and (d) 3D framework of **3** along *b*- and *c*- direction, respectively, (e) coordination environment of Co(II) (blue) and $pbdc^{2-}$ (violet), viewed as 5- and 3- connected nodes, respectively, (f) The hexagonal microporous channels along the *a*-axis, (g) the topological representation of binodal (3,5)-connected 3D single network. purple, $pbdc^{2-}$ ligand; blue, Co.

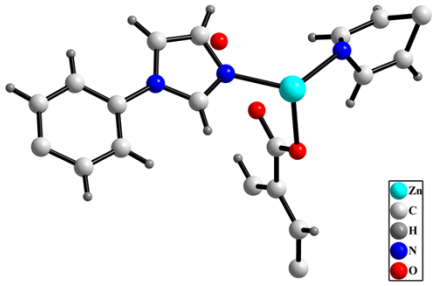

(a)

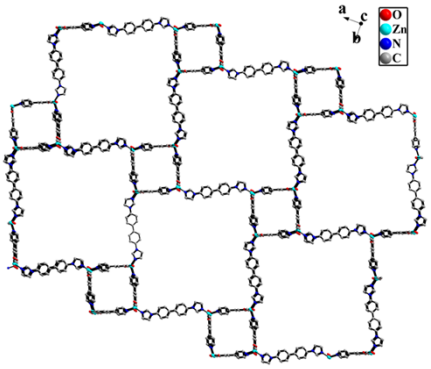

(b)

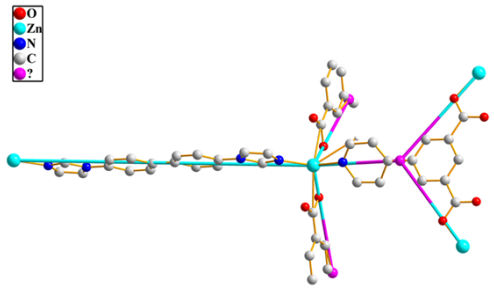

(c)

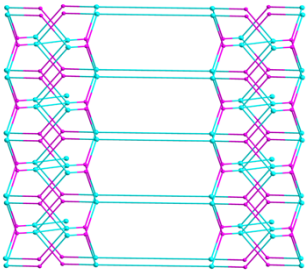

(d)

Figure S4. (a) The asymmetric unit of **4**, (b) 3D single framework of **4** along *c*- direction, (c) coordination environment of Zn(II) (blue) and $pbdc^{2-}$ (violet), viewed as 4- and 3- connected nodes, respectively, (d) the topological representation of binodal (3,4)-connected 3D single network. purple, $pbdc^{2-}$ ligand; blue, Zn1.

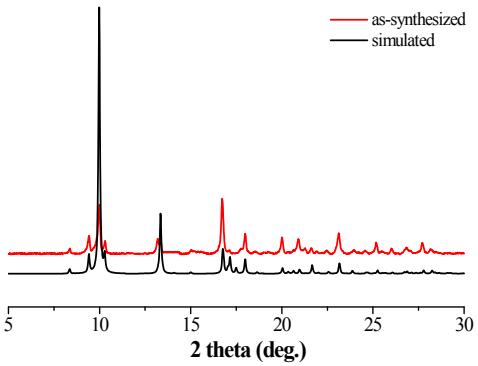

(a)

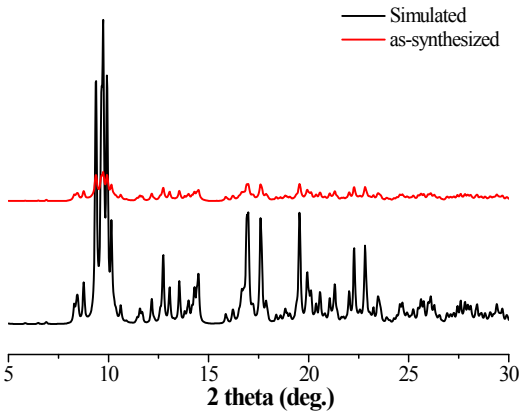

(b)

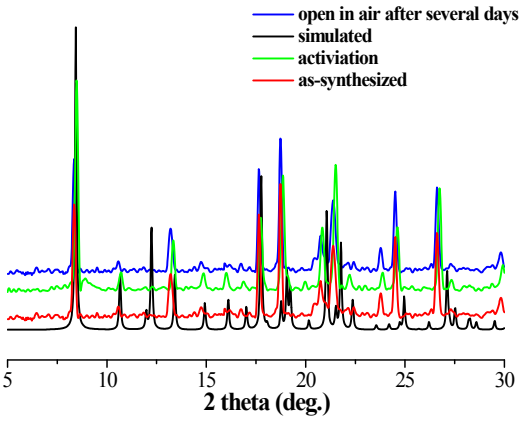

(c)

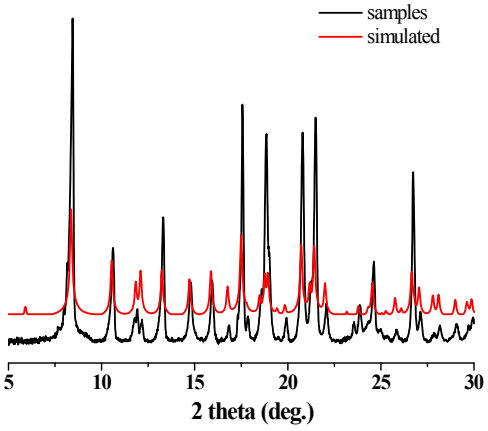

(d)

Figure S5. PXRD profiles for complexes **1** (a), **2** (b), **3** (c) and **4** (d). Simulated spectrum was calculated from the single crystal data.

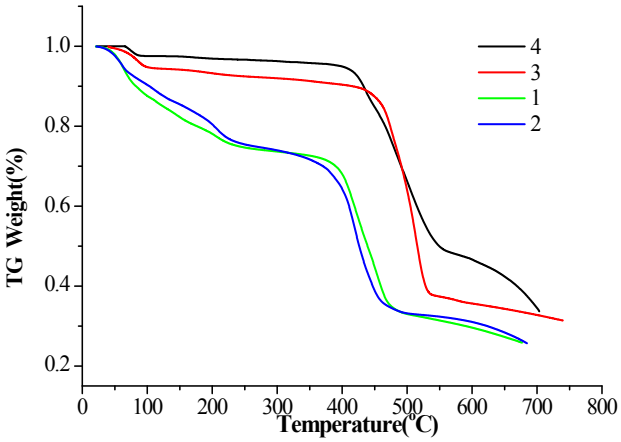

Figure S6. TG curves of complexes **1-4**.

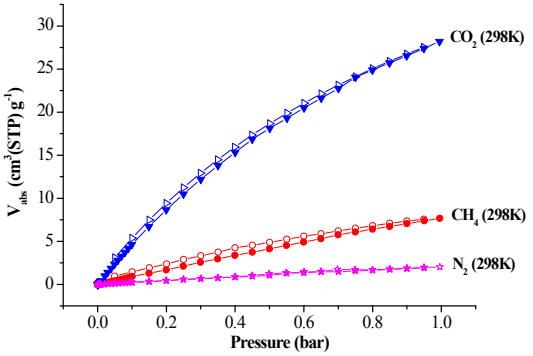

(a)

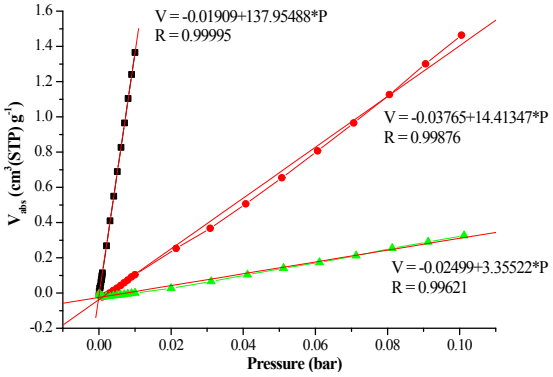

(b)

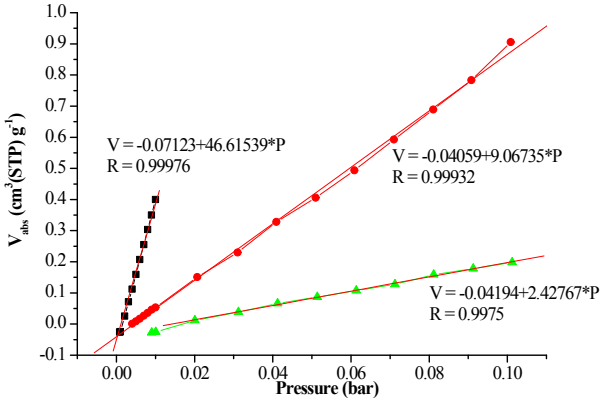

(c)

Figure S7. (a) Sorption isotherms for CO_2, CH_4, and N_2 at 298 K of desolvated **3** (adsorption and desorption branches are shown with filled and empty shape, respectively). (b) and (c) Evaluation of the initial slope in the Henry region of the sorption isotherms of CO_2 (square), CH_4 (circle), and N_2 (triangle) at 273 and 298 K, respectively. The ratios of the initial slopes allowed an estimation of the sorption selectivity.

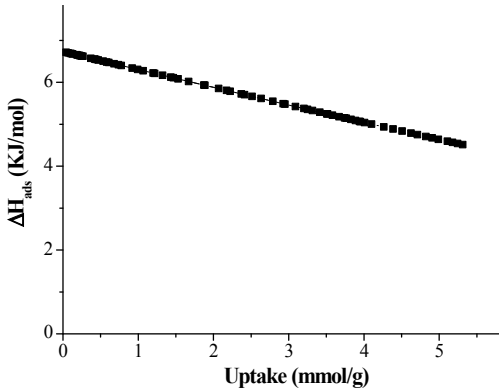

Figure S8. The isosteric heats of H_2 adsorption (Q_{st}) for desolvated **3**.

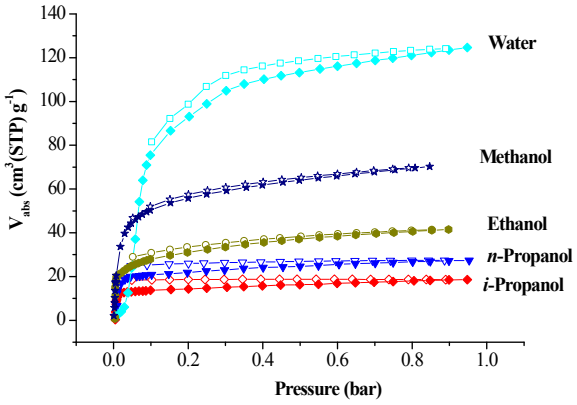

Figure S9. Water and alcohol vapor adsorption–desorption isotherms of the desolvated **3**: water, methanol, ethanol and *i*-propanol at 298 K, where filled and open shape represent adsorption and desorption, respectively.

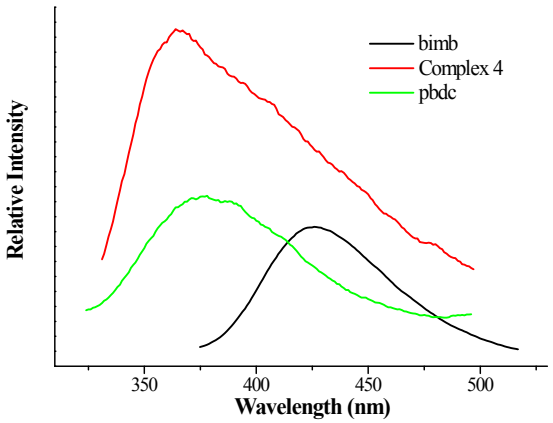

(a)

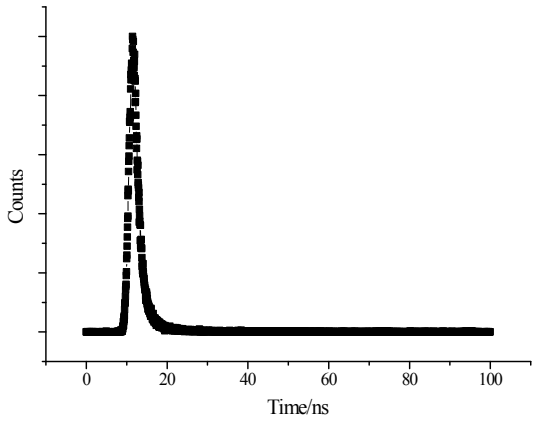

(b)

Figure S10. (a) The solid-state fluorescent spectra of **4** and free ligands at room temperature. (b) The emission decay lifetime of compound **4**.

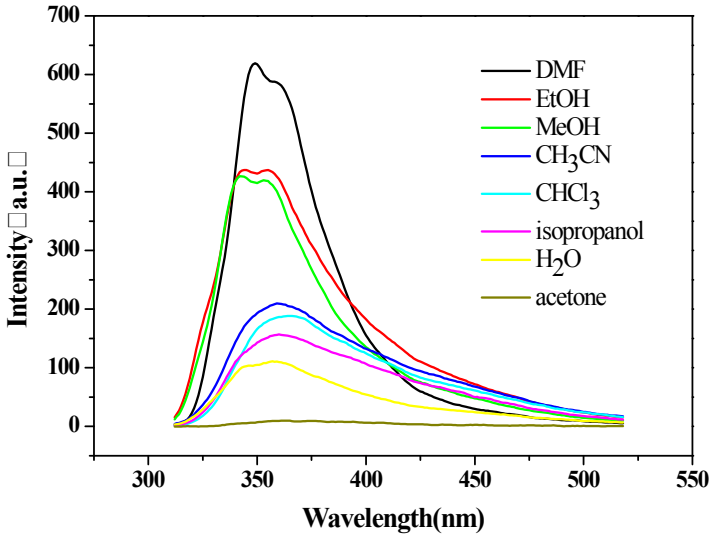

Figure S11. The PL spectra of **4** introduced to various pure solvent when excited at 290 nm.

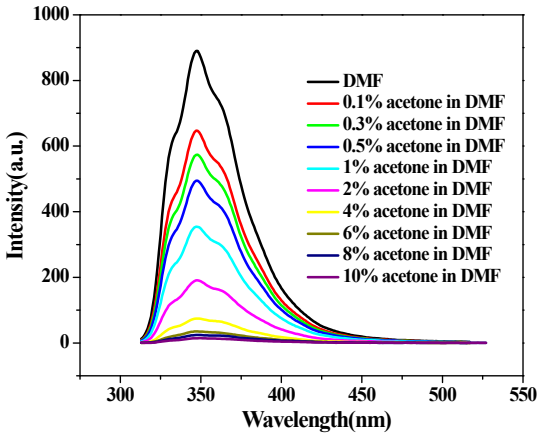

Figure S12. The PL spectra of **4** in the presence of various volumes acetone in DMF (excited at 290 nm).

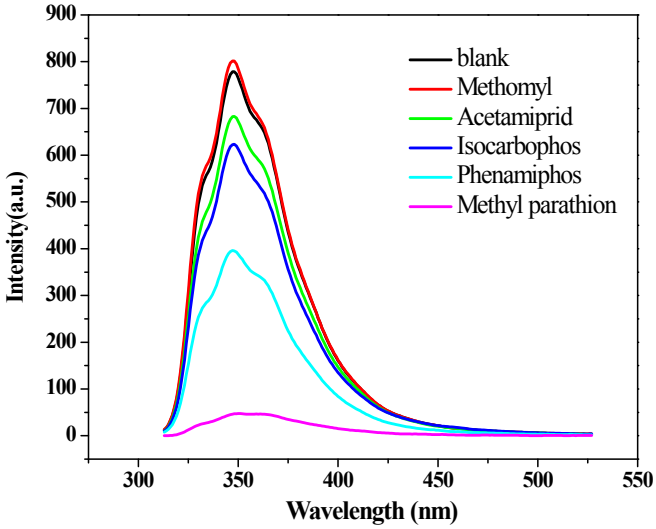

Figure S13. The PL intensities of **4** toward relevant pesticides with concentration of $1*10^{-3}$ M in DMF when excited at 290 nm.

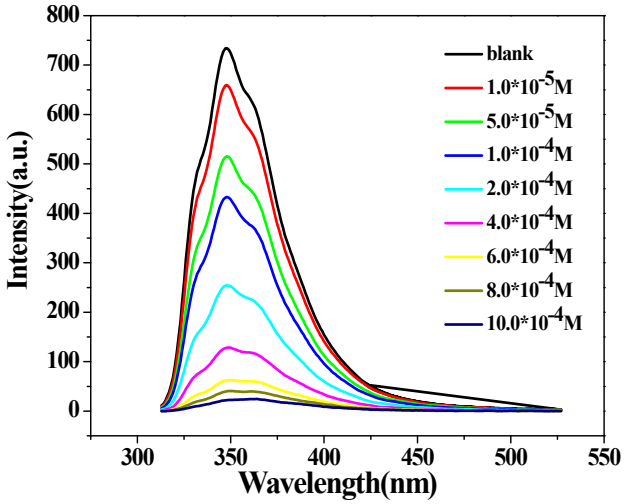

Figure S14. The PL intensity of **4** as a function of parathion–methyl at different concentrations in

DMF.

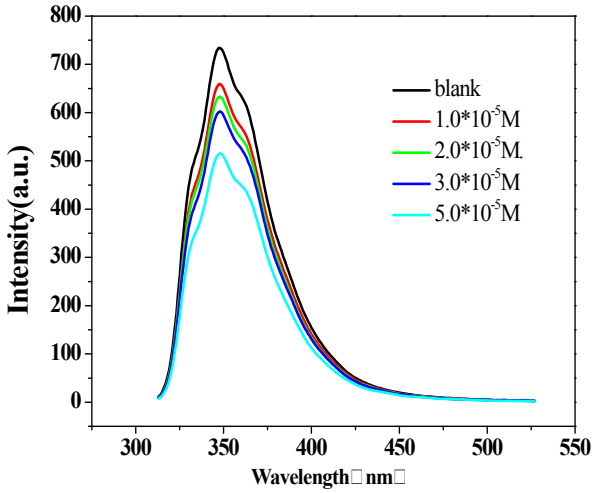

Figure S15. The PL intensity of **4** as a function of parathion–methyl at different concentrations in DMF.

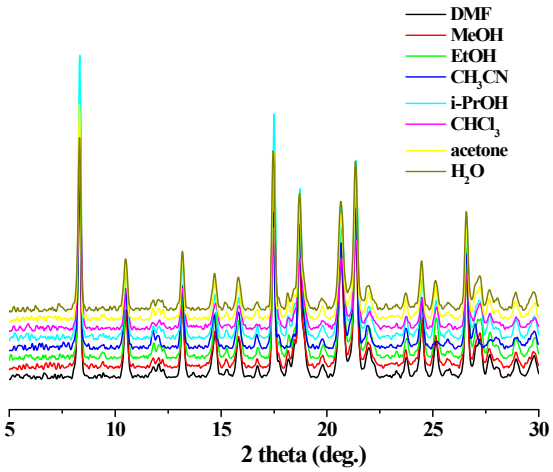

Figure S16. PXRD profiles for complexes **4** in different solvents.